transitions with a weak line at 22.235 GHz and much stronger lines at 183 GHz, 325 GHz.

The theory of molecular absorption has been considered by Van Vleck and Weisskopf [2]; Gross [3]; Zhevakin and Narrov [4]; Rosenkranz, [5]. Extensive comparisons [6] between the results of calculation and measurement have shown that in general, the attenuation due to oxygen is well described by the theory; for water vapour, however, there is a discrepancy between experiment and theory which may be accounted for by the inclusion of an empirical, non-resonant correction which depends on the square of the water vapour density. The origin of this effect is still not fully understood, although explanations have been sought in terms of hydrogen bonding of water molecules to form dimers [7,8] or of the water molecules clustering together [9] or in terms of errors in the line shape used in the calculations [10,11]. None of these, however, is yet able to explain adequately the observed attenuation by water vapour, and the empirical correction is still necessary to align the experiment with theory.

The calculations of zenith attenuation were made by Gibbins [12] based on microwave propagation model of Liebe [6] with a Van Vleck and Weisskopf [2] line shape. The results are shown in Figure 1.

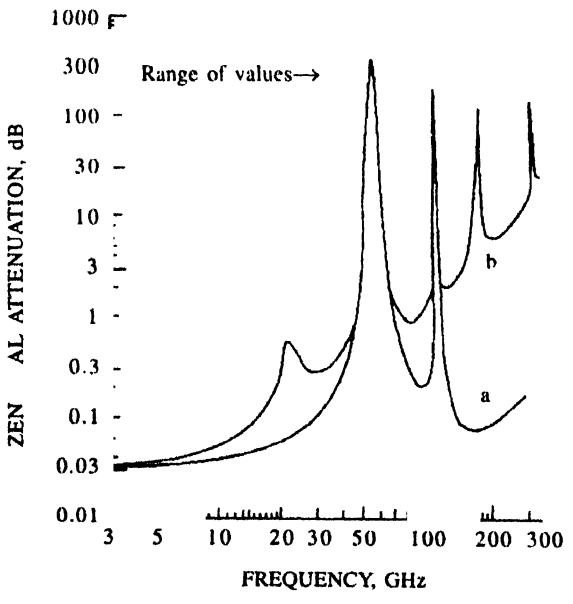

Figure 1. Total one-way zenith attenuation through atmosphere in the frequency range 3–330 GHz for :
(a) a dry atmosphere
(b) with water vapour (7.5 g/m³)
Ref : Gibbins [12].

However, the integrated water vapour content (water vapour content in a cylinder of base area 1 m² and of 10 km height and expressed in g/m²) not only controls the attenuation and group delay of microwaves and millimeter waves in satellite and line-of-sight (LOS) links but also introduces background radio noise in the links, thus affecting the signal-to-noise ratio significantly.

2. Radiosonde

Radiosonde measurements of temperature, pressure and humidity for altitudes upto about 16 km are the standard measurements of the world's weather services. For the purpose, the simplest technique is to use a hygrothermograph for humidity and temperature measurements and a microbarograph for pressure measurement. The pressure is, in fact, recorded by means of an aneroid capsule; temperature by means of an animal fibre whose length is dependent on humidity [13].

3. Modelling of meteorological parameters and attenuation coefficient

The water vapour density (g/m³) can be derived by using

$$\rho = \frac{e \times 1800}{8.31 \times T_D}, \tag{1}$$

where e is the water vapour pressure in hectopascals and is given by

$$e = 6.105\left[25.22\left(1-\frac{273}{T_D}\right) - 5.31 \log_e (T_D/273)\right]. \tag{2}$$

The absorption (cm⁻¹) of water vapour molecule at 22.235 GHz is given by Bhattacharya [14] as

$$\Gamma = 3.24\times10^{-4}\,\frac{P \exp[-644/T]^{\nu 2}}{T^{3.125}} \times\left[1+0.0147\frac{\rho T}{P}\right]\times\left[\frac{1}{(\nu+22.235)^2+(\Delta\nu)^2} + \frac{1}{(\nu-22.235)^2+(\Delta\nu)^2}\right] + 2.55\times10^{-8}\,\frac{\rho\nu^2\Delta\nu}{T^{3/2}}, \tag{3}$$

where, ν is the frequency in GHz, T is the kinetic temperature in K, $\Delta\nu$ is the pressure broadened line half-width parameter and is given by

$$\Delta\nu_b = 2.58\times10^{-3}\left[1+0.014\right]\frac{\rho T}{P}\Big]\frac{P}{(T/318)^{0.625}}\text{GHz}. \tag{4}$$

The attenuation rate due to water vapour monomer model in the atmosphere at 22.235 GHz may be estimated on the basis of eqs. (3) and (4).

The height distribution of the meteorological parameters such as atmospheric pressure, temperature, water vapour pressure and water vapour densities can be fitted with the following empirical relations :

$$e \text{ (mb)} = c_0 \exp(-m_1 h),$$

$$\rho \text{ (gm}^{-3}) = \rho_0 \exp(-m_2 h),$$

$$\rho \text{ (mb)} = \rho_0 \exp(-m_3 h),$$

$$T \text{ (K)} = T_0 m_4 h. \quad (5)$$

Besides these, the height distribution of absorption coefficient (dB/km) can also be fitted as

$$\alpha = \alpha_0 \exp(-m_5 h). \quad (6)$$

The scale factors of the above fitted equations for different seasons like pre-monsoon (March-May), monsoon (June-Sept), post-monsoon (Oct-Nov) and Winter (Dec-Feb) for Kolkata is presented in Table 1 [15].

Table 1. Scale factor of the fitted meteorological parameters.

Parameter	Season	Surface	Scale factor
Vapour pressure (mbar)	Pre-monoon	28.60	0.518
	Monsoon	39.90	0.473
	Post-monsoon	22.65	0.432
	Winter	16.94	0.479
Vapour density (g/m^3)	Pre-monoon	20.96	0.492
	Monsoon	28.77	0.450
	Post-monsoon	16.78	0.410
	Winter	12.76	0.470
Pressure (hpa)	Pre-monoon	1011.3	0.120
	Monsoon	1014.8	0.124
	Post-monsoon	1009.85	0.116
	Winter	1014.5	0.119
Temperature (K)	Pre-monoon	302.91	6.46
	Monsoon	302.50	5.68
	Post-monsoon	297.64	4.79
	Winter	294.10	5.13
Attenuation coefficient (db/km)	Pre-monoon	0.870	0.389
	Monsoon	1.173	0.342
	Post-monsoon	0.702	0.311
	Winter	0.540	0.374

The monthly variations of attenuation at 22.235 GHz in dB and the corresponding surface water vapour density ove Kolkata are shown in Figure 2. It is found that the nature of the monthly variations of these two parameters are the same and show a maximum in the months of July through August. The corresponding antenna temperature may be calculated by using the relation [16]

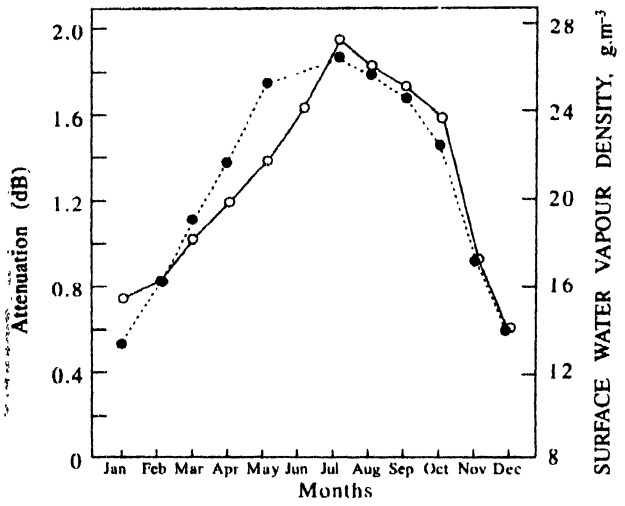

Figure 2. Monthly variation of calculated attenuation (dB) and the corresponding surface water vapour density (gm^{-3}).

$$A(\text{dB}) = 10 \log \frac{T_m - T_{\cos}}{T_m - T_a(f)}, \quad (7)$$

where $T_a(f)$ represents the antenna temperature at frequency f. T_m is the mean atmospheric temperature and is considered to be 275 K. It should be emphasised that T_m is found to be dependent on frequency and ground temperature [17].

Now, remembering eq. (5), we rewrite water vapour content as

$$W = H\rho \times \rho_0 \, 10^3 \text{ g/m}^2.$$

Now with a view to explore a relationship between the integrated water vapour content and the antenna temperature measured by the radiometer, a scatter plot between the two parameters has been drawn as shown in Figure 3. A regression analysis [15] has also been made and the best linear equation for Kolkata, is found to be

$$W \text{ (g/m}^2) = 612\, T_a + 16400,$$

where T_a is the antenna temperature in degree Kelvin. In this connection, it may be mentioned that the same regression analysis was done by Bhattacharya [14] for the Northern station at New Delhi and the best fit line for Delhi was

$$W \text{ (g/m}^2) = 588.23\, T_a - 2110.$$

The difference might originate from the climatic difference between the two stations, Kolkata and New Delhi.

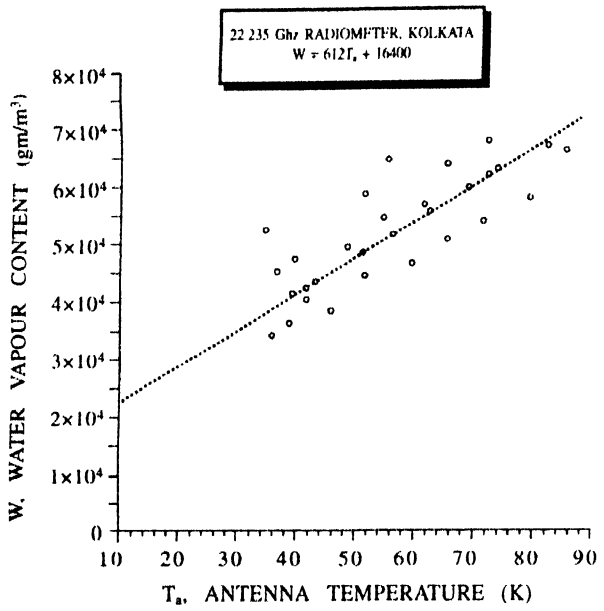

Figure 3. A scatter plot between antenna temperature and water vapour content over Kolkata.

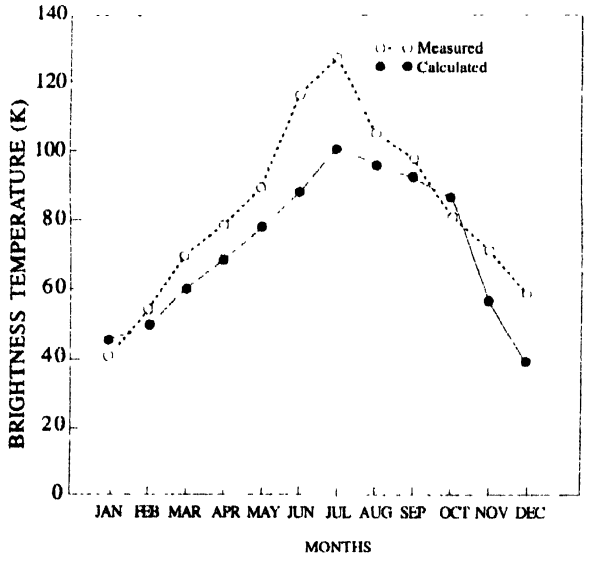

Figure 4. Monthly variation of estimated and measured brightness temperature (K) for clear air condition.

The Monthly variation of brightness temperature is presented in Figure 4 [15]. These also bear a maximum in the months of July through August.

However, according to Raina [18], it was found that during January-March, over Delhi, there is not much increase in water vapour. It starts rising from about the third week of May and continues to rise up to the end of August, with broad maxima during June-August. Again, over Jodhpur, it was found that the content of water vapour becomes maximum in August and falls off around the second week of September. But, on the other hand, water vapour content, over Srinagar, increases from the first week of February and attains maximum around July-August and then falls off from the first week of September.

Now by adopting the statistical regression analyses, it was found that the calculated values of attenuation against surface vapour density ρ_s, were fitted well by a linear relation

$$A\ (\text{dB}) = -0.1106 + 0.0686\ \rho_s, \qquad (8)$$

with a correlation coefficient of 0.096 and r.m.s. error of 0.116 (dB). However, the results of fitting to a second order polynomial show correlation coefficient and r.m.s. error of 0.96 and 0.116, respectively, and the relation is

$$A\ (\text{dB}) = -0.035 + 0.0529\ \rho_s + 3.8505 \times 10^{-14}\rho_s^2. \qquad (9)$$

From eqs. (5) and (6), it is found that both linear regression and second order polynomial regression give the same correlation coefficients and r.m.s. errors and hence linear regression relation may be accepted for the sake of mathematical simplicity.

The actual height distribution of water vapour density over Kolkata (lat. 22°32' N; 88°20' E) is shown in Figure 5(a), bearing a maximum value of about 25 g/m³ during the month of July. However, the radiosondes launched by

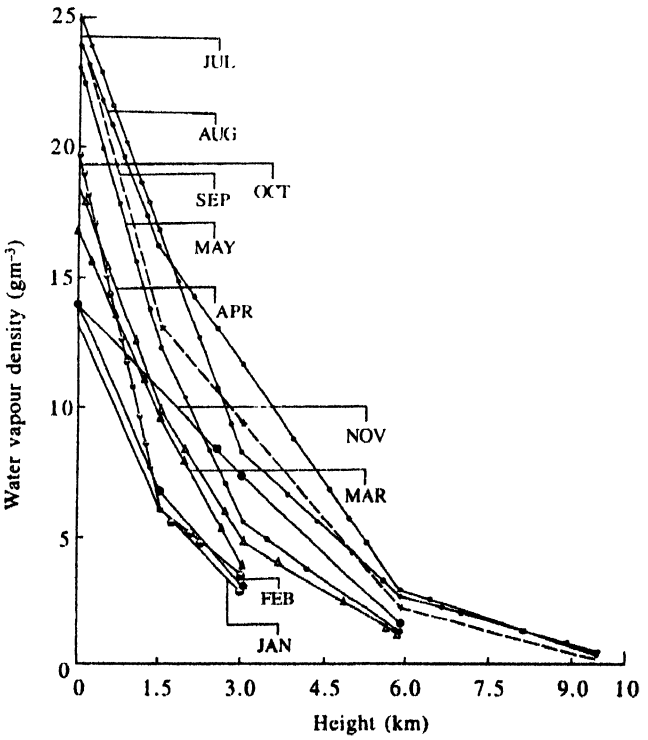

Figure 5(a). Monthly mean profiles of water vapour density over Kolkata using radiosonde data.

National Weather Service (NWS), USA, assigned to NASA Wallops Island Facility, during August 14, 1975 to August 25, 1975 reveals that maximum water vapour density is 11 g/m^3 [19], over Haystack observatory, in Westford, Massachusetts, USA. The data were then compared to find the accuracy by deploying a 22 GHz radiometer. The total uncertainty in temperature measurement was about 1.5 K in which the calibration error was 0.5k. This is presented in Figure 5(b).

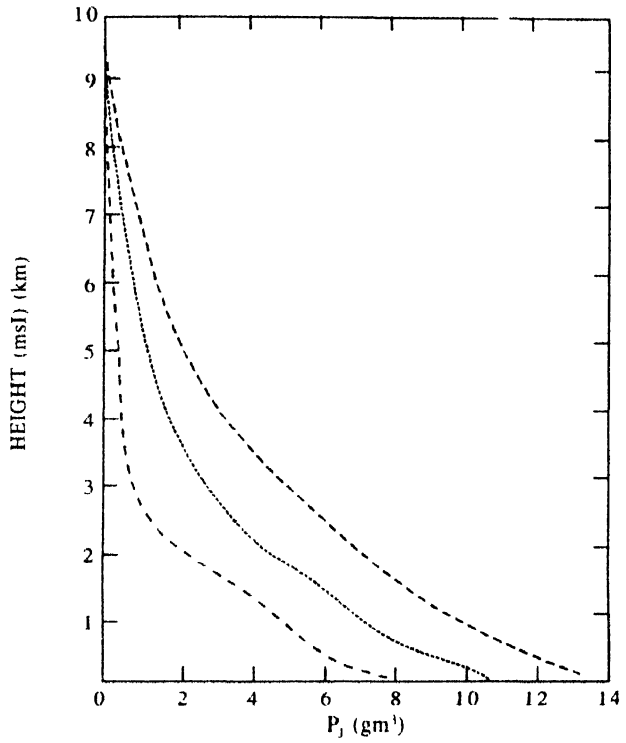

Figure 5(b). The mean profile of the water vapour from the data of 45 radiosonde launches at Haystack Observatory in August 1975. The dotted lines denote plus and minus standard deviation. Ref : Moran and Rosen [19].

It is to be mentioned here that while calculating the attenuation values in the microwave band, under prevailing meteorological conditions, several models currently available in literatures may be used. Table 2 presented here [20] is based on the model prescribed by Liebe [21], Waters [22] and Bhattacharya [14]. No appreciable difference amongst the results obtained by using different models is noticed. However, the model prescribed by Liebe is preferred for its good accuracy owing to the fact that Liebe has considered all the far-wing contributions to any desired frequency.

4. Significant heights for water vapour

The well known product-moment statistical formula may be employed in order to find out the correlation of the

Table 2. Comparative studies of attenuation using different models.

Month	Using Liebe model (dB)	Using Waters model (dB)	Unsing Bhattacharyay model (dB)
January	0.65339	0.665	0.6143
February	0.671	0.689	0.646
March	1.065	1.072	1.035
April	1.1869	1.193	1.164
May	1.391	1.390	1.386
Jun	1.724	1.703	1.716
July	2.036	2.027	2.0235
August	1.927	1.880	1.915
September	1.7084	1.676	1.683
October	1.4316	1.423	1.40
November	0.9403	0.9533	0.905
December	0.5899	0.610	0.5656

temporal variation of the water vapour density at different heights in the range 0–10 km, averaged over 12 and 24 h, with the variation of the integrated water vapour content. The results obtained over Digha (a coastal region) are shown in Figure 6. It is revealed that the correlation

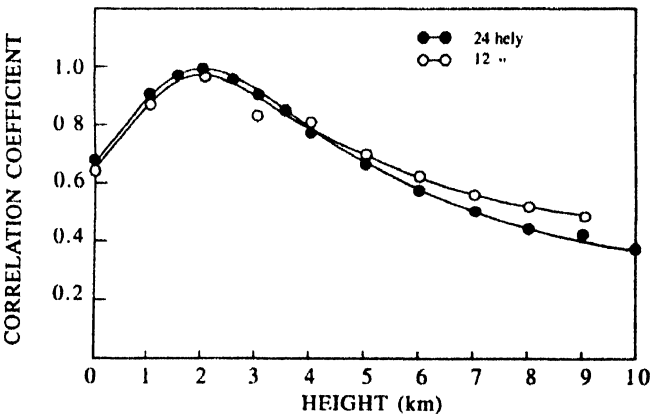

Figure 6. Correlation between the integrated water vapour content between the surface and a height of 10 km and water vapour density at several levels between the surface and a height of 10 km.

coefficient, between the integrated water vapour content (integrated between 0–10 km) and the water vapour density at different heights, is 0.65 at surface and it attains a broad maximum of about 0.95 at the heights (2 ± 0.5) km and drops to as low as about 0.4 for a height of 10 km for the averaging time of 12 and 24 h. For the 6-hour periods of averaging, however, there is no noticeable correlation. Thus, the heights over a range of ±0.5 km centred around 2 km are found to be the most significant heights representing the diurnal variation pattern of the integrated water vapour content [23].

A comparative study of the diurnal pattern of the integrated water vapour content and water vapour density at 2 km height has been made for 24 hours as well as 48 hours as shown in Figure 7. It is evident from this Figure that there exists a noticeable correlation in the case of 24 hourly averaging, but 48 hourly averaging to the same produces no appreciable correlation.

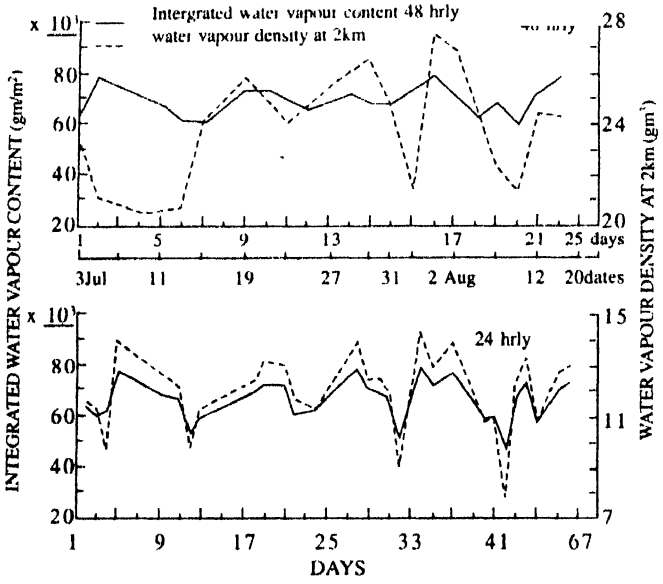

Figure 7. A comparative study of diurnal pattern of the integrated water vapour content and water vapour density at 2 km height for 24 hourly and 48 hourly averaging time.

The integrated water vapour content values for various heights from ground level is divided by the water vapour density found at 2 km height which exhibits the highest correlation as shown in Figure 6. The values, thus obtained, known as normalized values, W_N which are plotted against the average values of the heights up to which the densities are integrated. This technique has been reported for the monsoon data obtained for individual sites over the Indian subcontinent. The results obtained are shown in Figures 8(a) and 8(b). It is interesting to note that all these curves for the monsoon period exhibit a similar variation tending to attain a constant value near the average heights of 5 km which actually corresponds to a height of 10 km up to which the integration has been carried out. However, on furthering the regression analyses, it has been found that W_N fits with exponential model such as

$$W_N = K + ab^H, \tag{10}$$

where W_N is the normalized vapour density expressed in m at an average height H and K, a, b are the arbitrary constants.

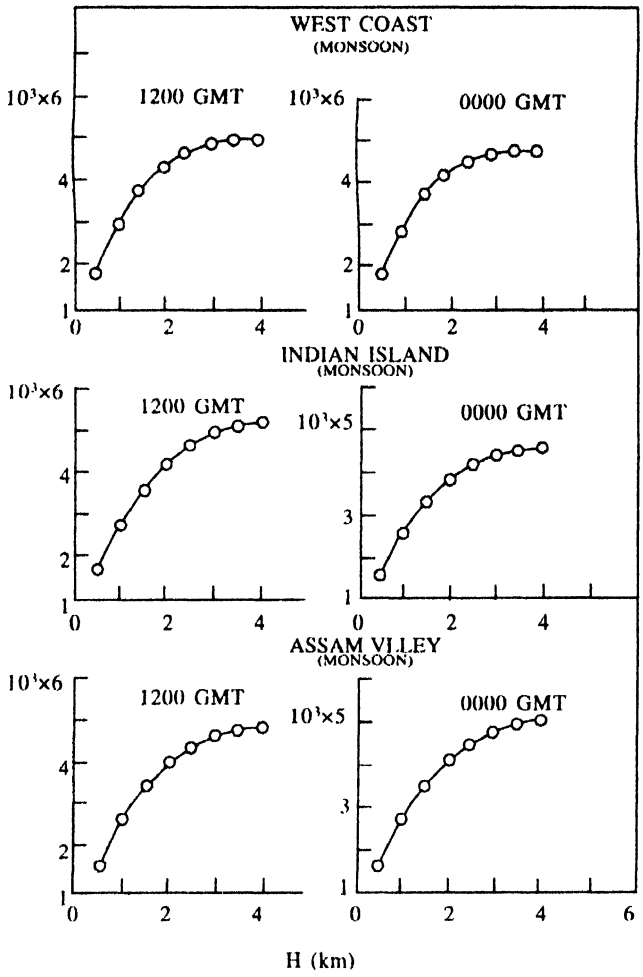

Figure 8(a). Ratio of integrated water vapour content to water vapour density at height of 2 km plotted against the height upto which densities have been integrated.

5. Time scale dependence of vertical distribution of water vapour

The observed maximum correlation coefficient between the water vapour content at 2 km height and the integrated water vapour content suggests that the integrated water vapour content is not affected by the temporal variations of water vapour density at the surface or that near 10 km height within the time scale of 12–24 hours. Hence, measurements around the 2 km height, which turns out to be the scale height, will be the most significant height in showing the temporal variations of the integrated water vapour content. It may be noted, however, that for a time resolution between 12 and 24 hours the correlation is good and, therefore, any transportation of the water vapour from the surface to the altitude at about 2 km must have been negligible effect within this time scale, in order that the observed lack of correlation of water vapour densities between the surface and the upper height regions

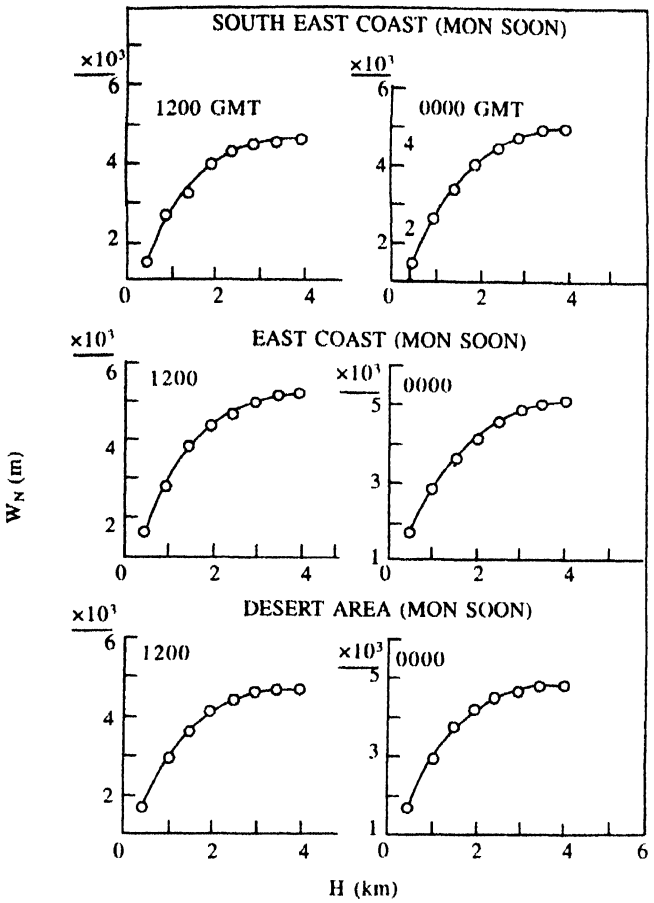

Figure 8(b). Same as in Figure 8(a).

may occur. If the time scale is increased to 48 hours, the integrated water vapour content is found to be poorly correlated with that at around 2 km height. This difference in behaviour in the nature of the correlation for a short (12-24 hours) and a long (48 hours) time scale suggests that the transportation of water vapour to higher altitudes occurred within a time scale greater than 24 hours. For a shorter time scale of 6 hours, again correlation is insignificant. This suggests the presence of finer and independent components of the temporal variation at various heights.

Further, the tendency of W_N, the normalized water vapor density distribution, to attain a constant value as shown in Figure 8 suggests that an increase in the altitude limit, up to which the water vapour densities are integrated, beyond 10 km will have a negligible effect on the integrated water vapour content.

It appears from the above discussions that the measurement of water vapour density at the significant height of 2 km alone may be adequate for obtaining a clear picture of the temporal variation of the integrated water vapour content in the atmosphere within the time scale of 12–24 hours. It is to be noted that for a longer time scale, the transportation of water vapour from the surface to higher altitudes is to be considered.

It may also be noted that the radiosonde data covers for the monsoon months only covering non-rainy periods as mentioned by Sen *et al* [23]. Due to rain, for which data were not available, there may be an appreciable rise in water vapor density at cloud heights (2–5 km) as well as at the heights encompassing rain.

The water vapour density at different height in the atmosphere may also be derived by using eqs. (1) and (2). It is revealed from the height distribution of water vapour density that in August, water vapour density attains the maximum value of 28.77 g/m^3 and is minimum in January and attains a value of about 11.80 g m^{-3} over the surface, as observed from the fitted curves of height distribution of water vapour density, over Kolkata (a tropical station), India [15].

Fitting of the density data with an exponential equation $\rho = \rho_0 \exp(-h/b)$ reveals that the monthly variation of scale height of water vapour becomes maximum during the month of July and August as is expected from the monthly variation of water vapour density over Kolkata. This is presented in Figure 9. Here, the water vapour scale height is defined as the height at which water vapour density becomes $1/e$ times the surface value.

The average value of calculated water vapour scale height over Kolkata (Figure 9), by using radiosonde data, is 2.45 km [15].

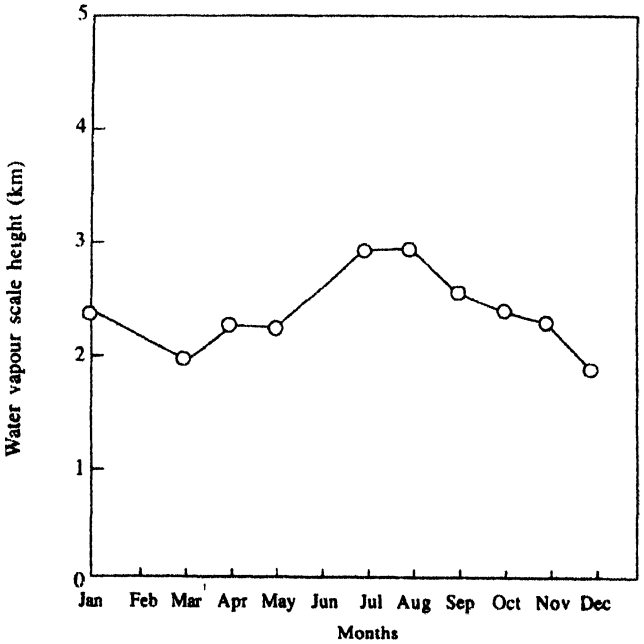

Figure 9. Monthly variation of estimated water vapour scale height over Kolkata (for clear conditions only).

However, referring back to Figure 4, the profile has approximately an exponential dependence with a scale height of 2.2 km, although the high altitude part decreases more slowly than an exponential [15]. Individual profiles deviated greatly from exponential dependence.

It is to be noted that the standard atmosphere is taken into consideration while representing eq. (5) may not be the actual representation. It may so happen that most of the times during the radiosonde studies, the sky may be overcasted with thin or thick clouds bearing non-precipitable liquid water. This, in turn, suggests the use of continuous monitoring of water vapour by deploying microwave radiometers.

6. Frequency dependence of water vapour distribution

In recent days, it is well known that the molecular resonance absorption or emission peaks are generally exploited for remote sensing of the atmospheric gases. Westwater and Decher [24] pointed out that the operation of a receiver at the resonance peak may lead to serious errors in retrieval mechanisms, due to pressure broadening of rotational lines. This pressure broadening effect is predominant at 22.235 GHz, where the line is relatively weaker as compared to the line at 183 GHz and the contribution of the wings of the higher frequency lines is also significant even at the peak of the water vapour resonance line [25]. Westwater [26] suggested some offset frequency of operation, such as, 21.0 or 24.4 GHz, as the operating frequency where the change in absorption caused by pressure broadening would be insignificant. At 21.0 GHz, the pressure broadened line is approximately two-thirds of its maximum emission intensity. Measurements at the offset frequency are, in fact, less sensitive to the distribution of water vapour with altitude but are better correlated with the integrated values of water vapour.

The pressure broadening effect is caused by pressure induced molecular collisions between H_2O and N_2 molecules and further increased by temperature of the medium. For places like Antarctica, where both the surface water vapour concentration and temperature are at lower values, the pressure broadening may not contribute significantly to affect the radiometric measurement even at the line centre 22.235 GHz and retrieval of water vapour density might be fairly accurate.

6.1. Choice of frequency :

In atmospheric remote sensing applications, the selected frequency should be very sensitive to the atmospheric parameters to be measured. Meeks and Lilley [27] and Hogg [25] discussed in detail the choice of frequency and prescribed some offset frequency away from 22.235 GHz as appropriate for all locations. However, calculation of brightness temperature [28] around 22 GHz water vapour line with surface temperature of 30°C and standard lapse rate

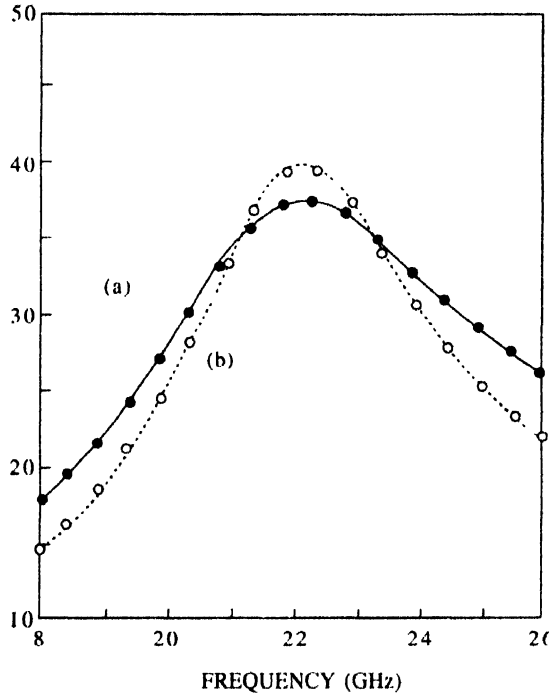

Figure 10. Line profiles of atmospheric water vapour for two different vertical distributions in standard atmosphere; (a) RH = 81.6% for 0 < H < 1000 m (open circles), (b) RH = 99% for 1000 < H < 3800 m (filled circles), Ref : Resch [28].

and with constant relative humidity 81.6% for $0 < h < 1000$ m and 99% for 1000 m $< h <$ 3800 m (Figure 10) shows that the height altitude profile is sharper than the low altitude profile, keeping water vapour content 2 g/m^2 same in both the cases. This suggests that if one wishes to maximise the signal from a given amount of vapour, then clearly the observation should be carried at 22.235 GHz. It is also clear from the Figure 10 that a single frequency measurement of brightness temperature near the half-power point of the line profile would provide the most accurate estimates. Moreover, as the line shape function remains almost unchanged with respect to height in regions with dry climate, the use of 22.235 GHz resonance line for radiometric measurement of water vapour density would be fairly accurate for regions like Antarctica.

Thus the choice of frequency depends on site, season and local meteorological condition. However, in selection of operating frequency, following criteria must be taken into consideration [29].

(i) The brightness temperature should be sufficiently sensitive to water vapour density and weakly sensitive to other atmospheric variables, *viz.* temperature, pressure and height.

(ii) For integrated water vapour measurement, the water vapour weighting function at the selected frequency should be height independent, *i.e.*, the weighting function should have a constant profile with height.

(iii) For vertical profiling of water vapour, the water vapour density weighting function should be sufficiently different with respect to height.

However, according to Raina [18], Figure 11 shows zenith antenna temperatures calculated at various frequencies for surface values of the water vapour at 5, 10, 15, 20 g/m^3, respectively. It is observed that for water vapour content of 5 g/m^3, antenna temperature varies between 2 K and 22 K. Likewise, variations for water vapour content at 10, 15 and 20 g/m^3 can be determined from Figure 11. Antenna temperature, as expected, is negligible below 10 GHz, but it increases with increase in frequency, thereafter becoming maximum at the water vapour resonance line of 22.235 GHz, and then decreasing with further increase in frequency. The variation of the antenna temperature with frequency at different values of surface water vapour content is shown in Figure 12. The maximum value of

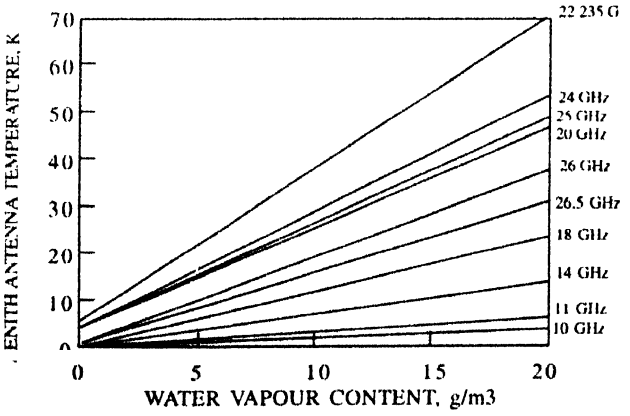

Figure 11. Zenith antenna temperature as a function of surface water vapour content. Ref : Raina [18].

antenna temperature is found to be around 75 K for water vapour content of 20 g/m^3 at 22.235 GHz and the minimum around 22 K at 5 g/m^3.

Figure 13(a) shows the variation of water vapour density weighting function at Kolkata estimated from radiosonde values. Weighting function profiles are drawn for frequencies at 21.0 and 22.235 GHz. The 21.0 GHz profile indicates a more or less constant trend with height which

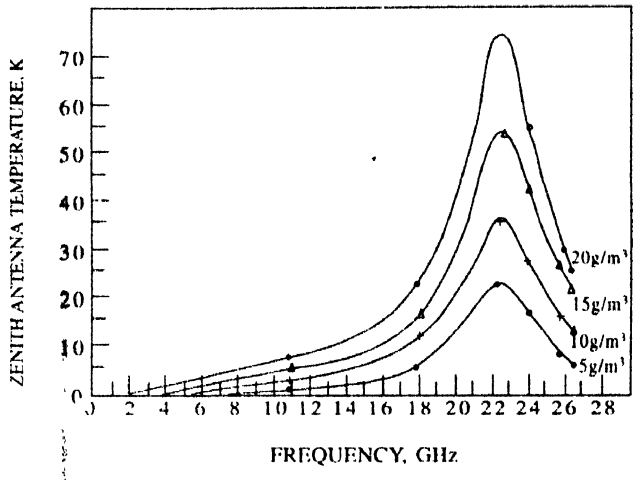

Figure 12. Variation of zenith antenna temperature with frequency for various value of water vapour content. Ref : Raina [18].

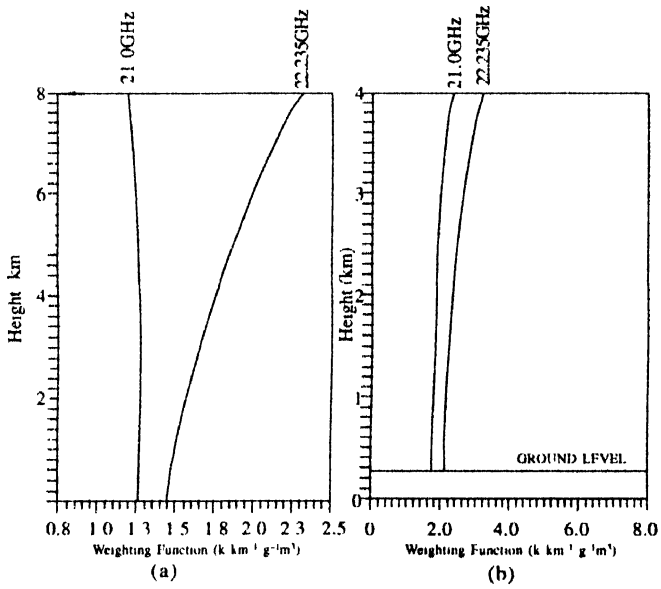

Figure 13(a). Variation of weighting function at 21.0 and 22.235 GHz. Over Kolkata. (b). Same as before but over Antarctica. Ref : Dutta and Sen [29].

favours the selection of 21.0 GHz for retrieval of integrated water vapour at tropical regions [29]. Figure 13(b) represents the estimated variation of the water vapour density weighting function with height at Antarctica up to 4 km. At any selected frequency in microwave band, the maximum absorption depends on (i) line strength factor, (ii) line width parameter [29]. Their values are decided mainly by collisions between H_2O and N_2 molecules. The effects of H_2O-H_2O and H_2O-O_2 collisions are very small and for Antarctica they are negligible. In Figure 13, the water vapour density weighting functions as estimated for Antarctica, at 21.0 and 22.235 GHz, are nearly constant through the first 3 km of height. It has been found that 70–80 percent of the attenuation is caused by the lower 3 km of atmosphere. Beyond 3 km, the weighting function tends to

vary slightly for both 21.0 and 22.235 GHz lines. The cause of bending may be due to the reason that radiosonde has poor accuracy in the relative humidity measurement, especially at high altitudes with low humidities. Apparently, both frequencies are suitable, as they exhibit similar trend, but 22.235 GHz may be preferred for its higher sensitivity to water vapour. Therefore, a 22.235 GHz radiometer can provide reasonably good information on integrated water vapour in regions with dry climate. Measurements at the line-centre frequency of 22.235 GHz have in fact, been reported by Decker *et al* [30].

6.2. Attenuation studies in 50–70 GHz band :

The 50–70 GHz band centered around the 60 GHz oxygen absorption band has drawn attention of many investigators apparently due to high absorption in the band allowing reliable communication. Near the ground level, the collisional or pressure broadening (self as well as foreign-gas broadening) results to merge together the large number of lines (nearly 44) near 60 GHz into a single broad absorption band. In fact, at high altitudes most of the transitions are clearly resolved in this millimeterwave band. In the frequency range 56–64 GHz, there exists the level of attenuation which is in excess of 10 dB/km at a pressure of 1013 mb, prevailing near the ground level. On either side of the strong oxygen absorption band 56–64 GHz (where attenuation rate is >10 dB/km), two bands may be considered amongst which, 50–55 GHz band is on the lower wing and the other one, 65–70 GHz is on the higher wing of strong oxygen absorption band where the attenuation is much less but depends markedly on the choice of exact frequency. Of these two bands the 50–55 GHz has been more widely studied as the instrumentation is more cost-effective at this band compared to that at 65–70 GHz where the rain attenuation is also much higher [31].

However, the influence of water vapour is small in the so-called oxygen band because of large frequency seperation between vapour and oxygen absorption. It is also known that the effect of clouds depend on the liquid water content and underlying surface emissivity which is analogus to vapour effect. Clouds can have appreciable water content throughout the troposphere and therefore can change the weighting function considerably and hence the brightness temperature also [32]. According to Grody [33], content of liquid water is found to decrease below the freezing point as a result of which clouds mainly affect the lowest sensing channels in the polar regions but on the other hand, clouds in the mid latitudes and tropics can affect the channels with higher peaking weighting functions [34]. But the clouds, over ocean can either increase or decrease the brightness temperature with no effect at 53.7 GHz. Over high emissivity lands, the clouds always decrease the brightness temperature [35]. It is to be mentioned here that the study in 50–70 GHz band is made useful for temperature sensing but the effect of water vapour and liquid water in the absorption band is to be studied rigorously over the place, in question. A sample plot of calculated values from NOAA 1981-82 data is shown in Figure 14 which shows that Kolkata and Srinagar being the two extreme locations, with widely varied local weather pattern, are having nearly same specific attenuation profile within the frequency band of 50–55 GHz in clear weather conditions. Even for the same location,

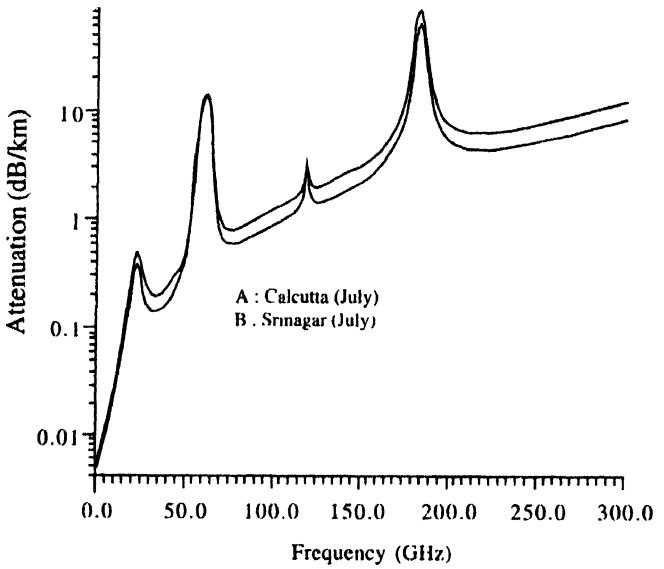

Figure 14. A sample plot of calculated specific attenuation *versus* frequency of propagation at Kolkata (lat 22°34'N, long 88°24'E) and Srinagar lat 34.06N, long 74.51E

Kolkata, at two discrete months, January and August of two extreme integrated water vapour contents of the atmosphere, 25.1 kg/m^2 and 66.50 kg/m^2 respectively, and corresponding to surface vapour contents of 11.2 gm/m^3 and 24.5 gm/m^3 respectively, the zenith opacity or the total integrated attenuation and specific attenuation varies respectively only within 0.5 dB and 0.2 dB/km for any frequency between 50 to 55 GHz (Figure 15(a),15(b)).

In this context, it is worthwhile to mention that during a theoretical study made over Indian subcontinent to identify the window frequency band, the 50–55 GHz band was found to be invariant, as its specific attenuation remain more or less invariant irrespective of locations. A sample plot is shown in Figure 16. For clarity, the propagational parameters in 50–70 GHz in clear air and in

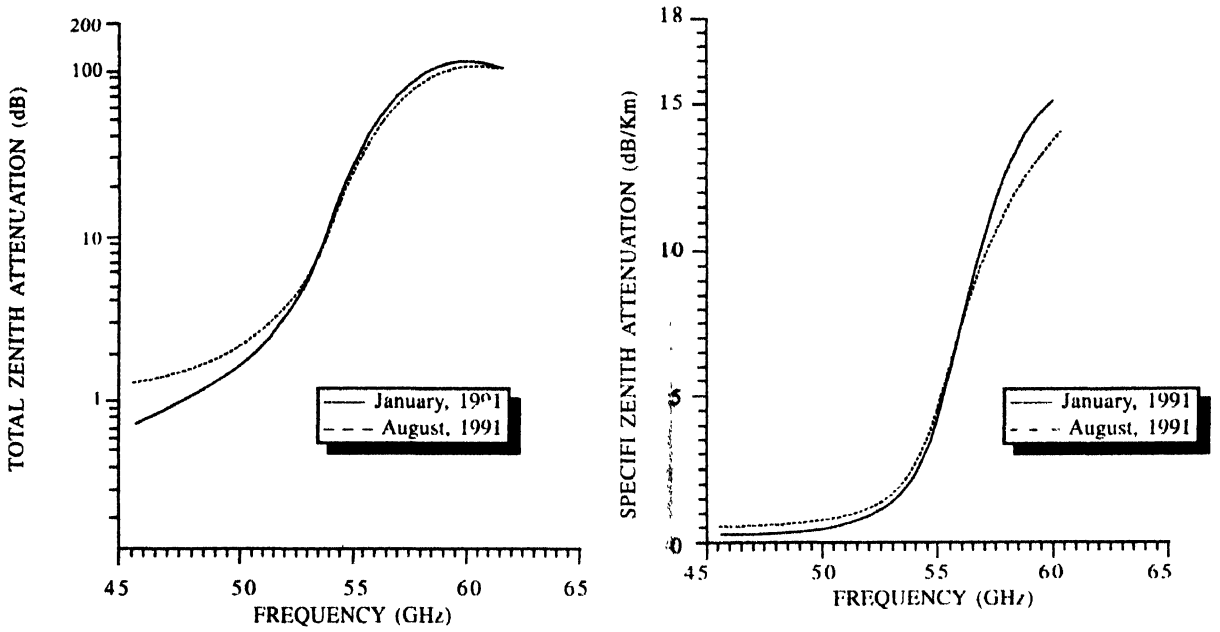

Figure 15. The variation of total zenith attenuation (a) and specific attenuation (b) in clear weather condition, with frequency in 50 to 55 GHz band as calculated from radiosonde data available for Kolkata.

the presence of hydrometeors whenever examined, [32] the distinct transition starts to occur at about 300 mb pressure in the range 57–63 GHz band. The sharp transition in this band is useful for communication. This seems to be plaucible because 58 GHz attenuation is 4 times larger than that at 59 GHz attenuation. But on the other hand, the situation seems to be the worst regarding the interference of the two very nearby channels.

India being a tropical country, most of its regions especially the coastal regions and to some extent the state adjoining these regions remain very much humid for a substantial period of a year. In the lower troposphere, the gaseous absorption, especially oxygen and water vapour dominates in the 30–300 GHz band. But as we know, the density of oxygen is constant unlike water vapour in the lower atmosphere, the oxygen absorption peak at 60 GHz would show consistency in its propagation behaviour unlike of that around water vapour absorption peaks. Thus, the oxygen band as absorption coefficient in the oxygen band is strongly dependent on the partial pressure of oxygen in the atmosphere and has a uniform and time-invariant mixing ratio, underlies the choice of oxygen band for retrieving purposes [36]. According to Westwater and Decker [37], the vertical profile of weighting function of 55.45 GHz decreases more rapidly with increasing height than the lower frequency (52.85, 53.85 GHz) profiles which implies that the surface layers within 1 km has the greater influence on 55.45 GHz and the least influence on 52.85 GHz. Also at 55.45 GHz, it is almost dominated by the first 3 to 4 km of the lower atmosphere. In contrast to this, the magnitude of the weighting function at 52.85 GHz remains significant up to 10 km height and even higher.

The calculations made by Karmakar *et al* [31], regarding clear air attenuation based on analytical equations developed by Ulaby *et al* [36], in the frequency band 50–55 GHz for its propagation through earth's atmosphere is presented in Figure 16. A more detailed description for millimeter wave absorption in the atmosphere can be

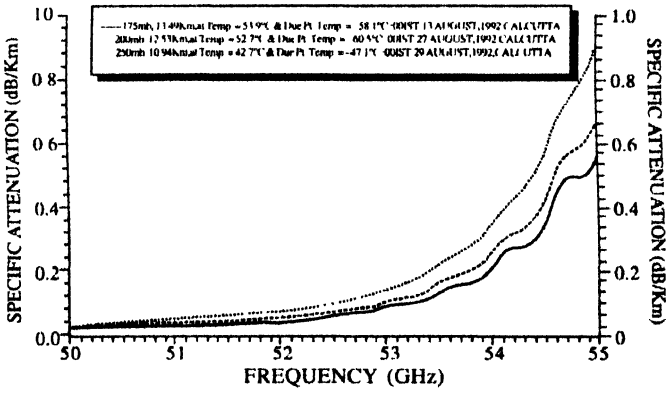

Figure 16. The plot gives the nature of the variation for the specific attenuation values at different frequencies between 50 to 55 GHz for three discreate radiosonde data sets (as indicated through inset) for Kolkata which shows that the existence of different absorption lines in the 60 GHz O_2 absorption band is more and more pronounced with the decrease of atmospheric pressure at high altitudes.

achieved by using MPM model [21]. Highest and lowest temperatures recorded for the surface atmospheric pressure (P = 1013 mb) are t = 34.6°C, dew point temperature t_d = 22.0°C over Chennai and for Srinagar are those t = 1.9°C and t_d = 2.1°C.

The absorption thus produced in dB/km (P = 1013 mb) as shown in Figure 17 from which it appears that the

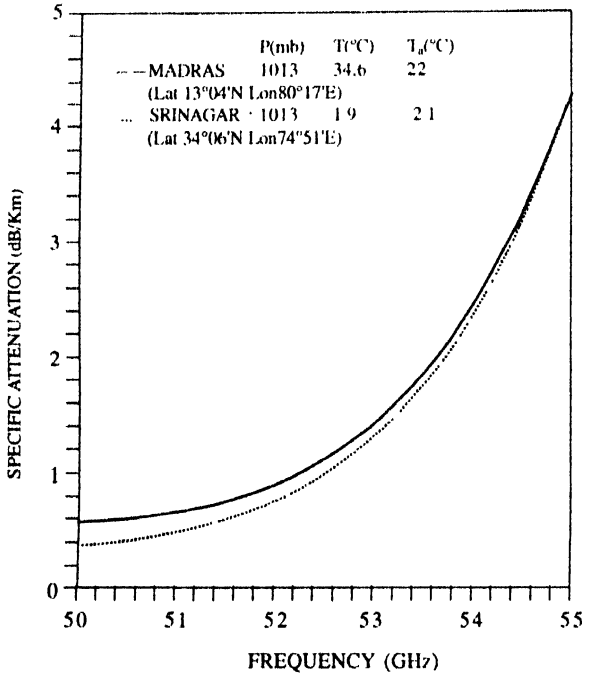

Figure 17. The plot shows the variational pattern of calculated (Liebe [21]) specific attenuation between 50–55 GHz at two extreme climatic conditions of two locations of India.

highest level attenuation occurs at 55 GHz which is approximately 10 times larger than that at 50 GHz. In this case, it is to be noted that during calculations, atmospheric pressure (P = 1013 mb) has not been altered but the temperatures range from 1.9°C to 34.6°C as is recorded over the whole of the country. Here, 1.9°C is found to be minimum and 34.6°C as maximum during the whole of the year over India. The difference in attenuation is pronounced, roughly more than 1 dB/km at 50 GHz and is going to decrease at higher frequencies, with an intersection at 53.75 GHz. This result signifies that this frequency *i.e.* 53.75 GHz is unique over Indian subcontinent for pressure sounder due to the fact that attenuation remains independent of temperature around this frequency.

It is also observed that the temperature dependence of attenuation, in terms of percentage change/degree centigrade from 1.9°C to 34.6°C, is linear over the frequency range 50–55 GHz. This is in conformity with the results that obtained by Gibbins [34].

According to Karmakar *et al* [31], the water vapour attenuation and oxygen attenuation were calculated separately and then summed up to find out the total attenuation coefficient for the frequency range 50-55 GHz. It is found there that the water vapour attenuation over Chennai ranges from 0.316 to 0.367 dB/km and corresponding oxygen attenuation ranges from 0.226 to 3.765 dB/km for temperature t = 22.0°C. But, on the other hand water vapour attenuation over Srinagar ranges from 0.077 to 0.09 dB/km and oxygen attenuation from 0.338 to 4.324 dB/km for temperature t = 1.9°C , for the frequency range 50-55 GHz. It is clearly understood from the results that lower the dew point temperature, larger is the dominance of oxygen attenuation over the total attenuation. For example, at 55 GHz ratio of water vapour and oxygen attenuation over Chennai and Srinagar comes out to be 0.097 and 0.020 respectively which clearly signifies the dependence of dew-point temperature on total attenuation coefficient also. Also it is seen that attenuation varies from 0.45 dB/km to 4.5 dB/km for 50 GHz and 55 GHz respectively.

6.2.1. *Possible application in 50–70 GHz band*

With the discussions made in the previous articles it is seen that the oxygen band may be precluded from communication point of view. But this large attenuation provided by the atmosphere gives additional isolation which may be used by the communication engineers for mobile networking in rural or urban areas. This oxygen band may also be used for traffic control and vehicular collision avoidance radar. It has been well discussed that the distinct transition starts to occur in frequency band 57–63 GHz at about 300 mb pressure. In this band attenuation ranges from 1 dB to 100 dB at the central frequency *i.e.* around 60 GHz. Apparently this large attenuation does not favour the earth/space communication.

It is also observed by Karmakar *et al* [31] that the effect of variation of water vapour content in the atmosphere does not affect much on attenuation due to gaseous molecules in 50–55 GHz band at a particular location over Indian subcontinent. This is primarily could be the major reason for exploiting this band for communication purposes over the Indian subcontinent.

7. Attenuation studies at 94 GHz

In the neighbourhood of 94 GHz, the absorption due to water vapour is not only contributed by two distinct rotational lines at 22.235 and 183.31 GHz together, but also is contributed by non-resonant absorption processes. The major contribution of water vapour attenuation at 94 GHz

is, however, due to rotational absorption lines of 22.235 and 183.31 GHz. Thus, the attenuation due to water vapour at 94 GHz may be estimated by summing up those contribution of two aforesaid absorption lines. The contribution of attenuation coefficient at the upper wing of 22.235 GHz and those at lower wing of 183.31 GHz at different heights were summed up which, in other words provide the attenuation rate at 94 GHz [38]. The contribution of higher frequency resonant lines have been neglected.

7.1. Theoretical consideration :

The attenuation rate α (cm^{-1}) due to water vapour in the atmosphere at 22.235 GHz may be calculated on the basis of the eq. (1) through (4).

Further, the expression for attenuation rate at 183.31 GHz water vapour line $\alpha_{183.31}$ using the appropriate term values [39] and temperature exponent [40] is shown by Croom [41]

$$\alpha_{183.31} = \frac{0.646 N\nu^2 \exp(-200/T)}{10^{28} \quad \pi^{3/2}}$$

$$[\Delta\nu_{p(183)}/\{(\nu - \nu_{00})^2 + (\Delta\nu_{p(183)})^2\} + \Delta\nu_{p(183)}/\{(\nu - \nu_{00})^2$$

$$+(\Delta\nu_p(183)^2\}] + \frac{1.8}{10^{32}} \frac{N\nu^2(\Delta\nu_{p(183)})}{T^{3/2}} \qquad (11)$$

where ν_{00} in GHz, is the resonance frequency for 183.31 GHz line, ν and T bear the same significance as mentioned earlier and N represents the number of water vapour molecules per cubic centimeter and is given by :

$$N = \frac{\rho}{18} \times 6.023 \times 10^{17} \qquad (12)$$

Here ρ is the water vapour density in g/m^3.

The line half width parameter for 183.311GHz, $\Delta\nu_{p(183)}$, as given in Waters [42] can be represented as

$$\Delta\nu_{p(183)} = 2.68\ [P/101013]$$

$$[300/T]^{0.649}[1 + 0.0203\rho T/P]. \qquad (13)$$

At 94 GHZ, the water vapour attenuation could be assumed primarily due to the contribution of resonant and non-resonant parts of 22.235 and 183.31 GHz water vapour absorption spectra as given in eqs. (3) and (11) respectively and hence is calculated accordingly. It may be mentioned here that the contribution from the lower wing of the water vapour line at 325.153 GHz is found to be much less compared to the attenuation value at 94 GHz. The attenuation contributions at 94 GHz due to 325.153 GHz as well as due to other high resonant absorption lines in near infrared have not, therefore, been taken into account.

7.1.1. Computation of 94 GHz attenuation from radiosonde data

The radiosonde data for the months of July and August 1979 during the MONEX (Monsoon Experiment) period over Digha (lat 21°41'N; long 87°40'E), a coastal region near the Bay of Bengal and that for the same period for Kolkata, four times a day at 00.00, 06.00, 12.00 and 18.00 GMT were used to calculate N, ρ, e and $\Delta\nu_{p(22)}$ and $\Delta\nu_{p(183)}$ and finally to obtain the value of α at 94 GHz as a function of altitude. Tables 3 and 4 show sample tabulations for all the parameters for a particular day and time for two different years over Kolkata and Digha. The variation of line width parameters of 22.235 and 183.31 GHz respectively, $\Delta\nu_{p(22)}$ and $\Delta\nu_{p(183)}$, with height is shown in Figure 18.

7.2. Results :

Computational techniques have been employed in order to find out the different parameters at different heights four times a day. The following striking features are revealed from the computation :

(i) The 94 GHz specific attenuation values as obtained from 22.235 GHz and 183.31 GHz absorption lines are of nearly same order of magnitude for a set of meteorological data of a particular height.

(ii) The 94 GHz attenuation value as obtained from 183.31 GHz is on an average 1.4 times that obtained from 22.235 GHz line (refer to last coloumn of Tables 3 and 4). Hence the following empirical relation can be formulated : Thus, we have,

$$\alpha_{94} = (\alpha_{94})_{22} + (\alpha_{94})_{183},$$

where α_{94} is the total water vapour attenuation due the contributions from 22.235 and 183.31 GHz collectively and $(\alpha_{94})_{22}$ and $(\alpha_{94})_{183}$ are the non-resonant water vapour attenuation contributions at 94 GHz.

Now referring to Table 3, it clearly indicates that

$$(\alpha_{94})_{183} \cong 1.4 \times (\alpha_{94})_{22},$$

Therefore,

$$\alpha_{94} = (\alpha_{94})_{22} + 1.4 \times (\alpha_{94})_{22} = 2.4 \times (\alpha_{94})_{22}. \qquad (14)$$

The above relation reveals an interesting result, *i.e.*, the water vapour attenuation at 94 GHz is 2.4 times that contributed from the line at 22.235 GHz alone. Now, by using eq. (14), a plot of α_{94} at respective heights is represented in Figure 19. The plot assumes a best fit

Table 3. Radiometeorological data for Kolkata of 05.00 hr 19 July 1991 along with water vapour absorption lines 22.235 and 183.31 GHz parameters.

Height (km)	Pressure (mb)	Temp. °C	Dew point °C	Vapour pressure (mb)	Vapour density (gm/m^2)	$\Delta\nu_{22}$ (GHz)	$\Delta\nu_{183}$ (GHz)	No. of molecules (cc)	$(\alpha_{94})_{22}$ dB/km	$(\alpha_{94})_{183}$ dB/km	$(\alpha_{94})_{22}$ $+(\alpha_{94})_{183}$ dB/km	$\frac{(\alpha_{94})_{183}}{(\alpha_{94})_{22}}$
0	1000	29.8	26.1	34.28	24.81	3.164	3.030	8.304E+17	0.62	0.87	1.49	1.40
0.465	950	27.8	27.6	37.49	27.00	3.067	2.944	9.036E+17	0.66	0.93	1.59	1.40
0.945	900	24 6	22.6	27.73	20.31	2.843	2.179	6.795E+17	0.47	0.66	1.13	1.40
1.446	850	22.6	21.1	25.27	18.60	2.686	2.568	6.226E+17	0.41	0.57	0.98	1.40
1.974	800	19.0	18.6	21.62	16.05	2.523	2.409	5.370E+17	0.34	0.47	0.81	1.40
2.528	750	15.4	15.4	17.63	13.23	2.355	2.245	4.427E+17	0.26	0.37	0.64	1.40
3.112	700	12.5	11.9	14.03	10.66	2.185	2.080	3.566E+17	0.20	0.28	0.48	1.40
3.734	650	10.0	8.0	10.80	8.32	2.016	1.917	2.784E+17	0.15	0.20	0.35	1.40
4.397	600	7.1	4.6	8.55	6.67	1.857	1.746	2.231E+17	0.11	0.15	0.26	1.40
5.110	550	3.6	1.2	6.73	5.31	1.704	1.616	1.777E+17	8.17E-02	0.11	0.20	1.40
5.880	500	-0.2	-2.5	5.15	4.12	1.551	1.471	1.379E+17	5.89E-02	8.28E-02	0.14	1.41
6.718	450	-5.1	-6.3	3.88	3.15	1.403	1.329	1.054E+17	4.18E-02	5.89E-02	0.10	1.41
7.635	400	-9.9	-12.1	2.48	2.06	1.250	1.184	6.892E+16	2.50E-02	3.52E-02	6.02E-02	1.41
8.653	350	-15.9	-19.3	1.38	1.18	1.101	1.041	3.955E+16	1.30E-02	1.84E-02	3.15E-02	1.41
9.794	300	-25.5	-29.9	0.55	0.49	0.958	0.906	1.642E+16	4.97E-03	7.07E-03	1.20E-02	1.42
11.09	250	-34.9	-40.9	0.19	0.18	0.185	0.771	6.047E+15	1.64E-03	2.35E-03	3.99E-03	1.43

Table 4. Radiometeorological data for Digha (lat 21°41'E long 87°40'N) of 05.00 hr 19 July 1979 (MONEX PERIOD) along with water vapour absorption lines 22.235 and 183.31 GHz parameters.

Height (km)	Pressure (mb)	Temp. °C	Dew point °C	Vapour pressure (mb)	Vapour density (gm/m^3)	$\Delta\nu_{22}$ (GHz)	$\Delta\nu_{183}$ (GHz)	No. of molecules (cc)	$(\alpha_{94})_{22}$ dB/km	$(\alpha_{94})_{183}$ dB/km	$(\alpha_{94})_{22}$ $+(\alpha_{94})_{183}$ dB/km	$\frac{(\alpha_{94})_{183}}{(\alpha_{94})_{22}}$
0.471	950	26.3	24.0	30.22	22.03	3.001	2.871	7.371E+17	0.53	0.75	1.28	1.40
0.947	900	23.6	19.2	22.45	16.63	2.794	2.665	5.565E+17	0.38	0.53	0.91	1.40
1.443	850	20.7	16.4	18.80	14.06	2.629	2.504	4.705E+17	0.31	0.43	0.73	1.40
1.996	800	17.8	13.4	15.47	11.70	2.465	2.345	3.915E+17	0.24	0.34	0.58	1.40
2.512	750	14.7	9.6	12.03	9.22	2.30	2.18	3.085E+17	0.18	0.25	0.43	1.40
3.1	700	11.0	5.7	9.23	7.17	2.14	2.03	2.398E+17	0.13	0.19	0.32	1.40
3.710	650	7.9	2.3	7.29	5.73	1.99	1.88	1.918E+17	0.10	0.14	0.24	1.40
4.364	600	4.2	-1.3	5.62	4.48	1.84	1.74	1.498E+17	740E-02	0.10	0.18	1.40
5.068	550	0.1	-5.5	4.12	3.34	1.69	1.60	1.116E+17	5.17E-02	7.27E-02	0.12	1.40
5.826	500	-3.6	-10.1	2.90	2 39	1.54	1.45	7.998E+16	3.45E-02	4.85E-02	8.29E-02	1.41
6.65	450	-8.4	-15.8	1.84	1.55	1.39	1.31	5.182E+16	2.07E-02	2.92E-02	4.99E-02	1.41
7.560	400	-13.9	-20.9	1.21	1.04	1.25	1.18	3.483E+16	1.29E-02	1.82E-02	3.10E-02	1.41

negative exponential decay curve which is represented as

$$\alpha = C_0 \exp\{ - h/C_1\} \quad (15)$$

where C_0 and C_1 are regression constants. The scale height C_1 is found to be 1.93 and 2.68 km for Digha and Calcutta respectively. This again shows that even the use of same data set of the same day for two different years 1978 and 1991 give different scale heights for 94 GHz specific attenuation as because water vapour concentrations are different for two locations. All these results are obtained during the most humid monsoon months over the areas where water vapour density attains almost the highest values over the Indian subcontinent.

8. Water vapour distribution over the Indian subcontinent

From the meteorological point of view the whole of the country is divided into two categories and they are namely [43] :

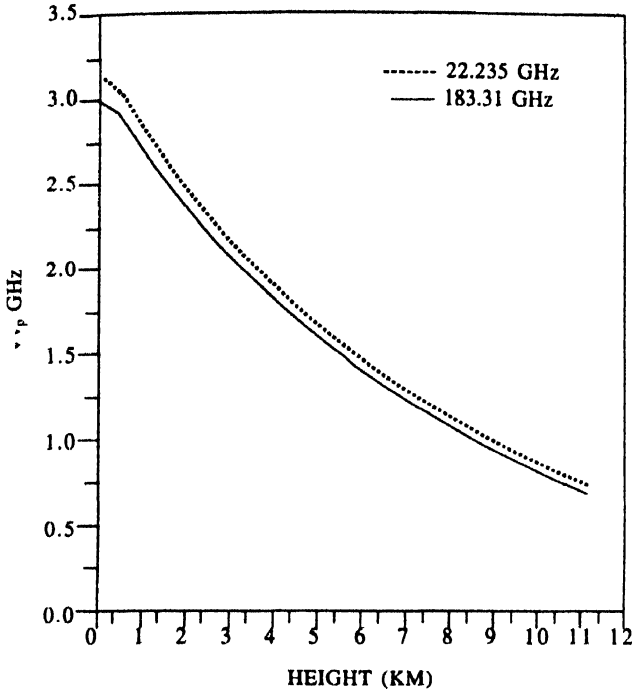

Figure 18. Plot show the variation of linewidth parameters ($\Delta\upsilon\rho$) of H_2O molecule at the absorption line frequencies 22.235 and 183.31 GHz. Ref : Mitra [35].

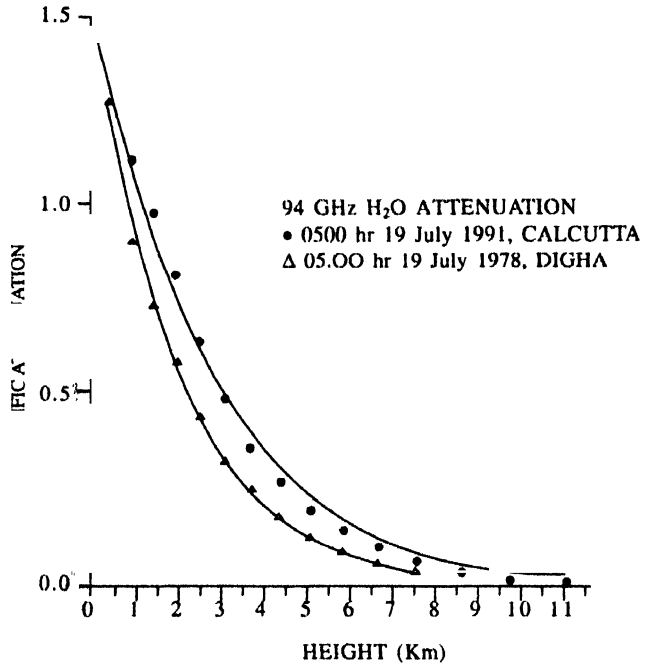

Figure 19. The plot shows the specific attenuation (α) due to water vapour at 94 GHz as calculated from 22.235 and 183.31 GHz water vapour absorption lines (from radiosonde data of 19 July 1991 for Kolkata and 19 July 1978 [MONEX] for Digha (long 87°40'E, lat 21°41'N).

(a) (i) Indian Island,

(ii) South East Coast,

(iii) South West Coast,

(iv) East Coast,

(v) West Coast and

(b) (vi) Northern Plane,

(vii) Central Plane,

(viii) Western Plane,

(ix) Southern Plane,

(x) Desert Area and

(xi) Assam Valley.

Now by using "The Atlas of Tropospheric water vapour over the Indian subcontinent" published by National Physical Laboratory, New Delhi, India, compiled from the data collected by the India Meteorological Department on a routine basis over sixteen stations during 1968-71, through 1000 mb to 50 mb pressure level, the water vapor distribution may be found out. For this purpose, a very simple procedure of integration of, $\int_0^h \rho\,(h)\,dh = W$ may be adopted. An attempt has been made by Sen and Karmakar

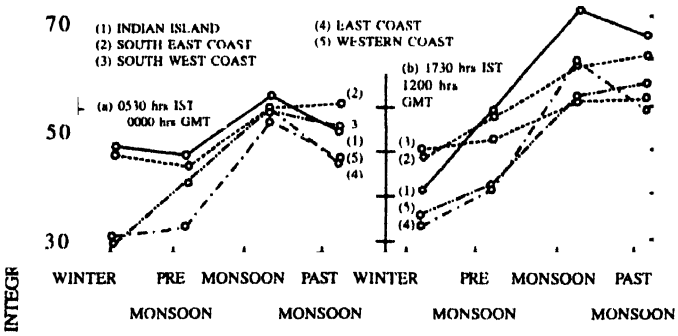

Figure 20(a,b). Variation of integrated water vapour content over coastal regions.

[43] to find out the integrated water vapour content over whole of the country, India (a tropical country).

The seasonal variation of the integrated water vapour content at 0530 IST (0000 GMT) and 1730 IST (2230 GMT) over the coastal regions of India are shown in Figures 20(a) and 20(b) respectively while those for the planes, the distributions are presented in Figures 21(a) and Figure 21(b) respectively. The corresponding attenuations at 22.235 GHz are presented in Figure 22.

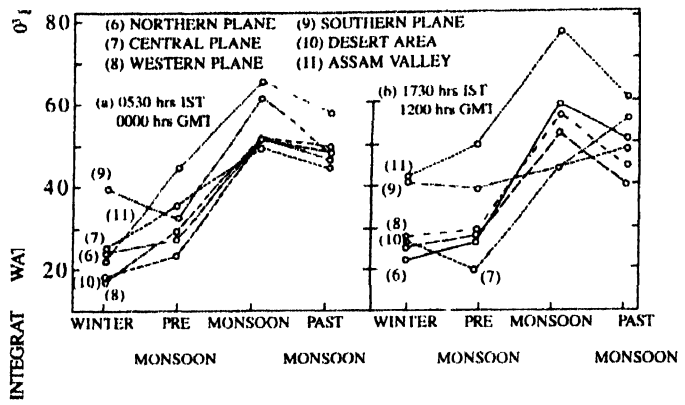

Figure 21(a,b). Same as befor but over planes and valley.

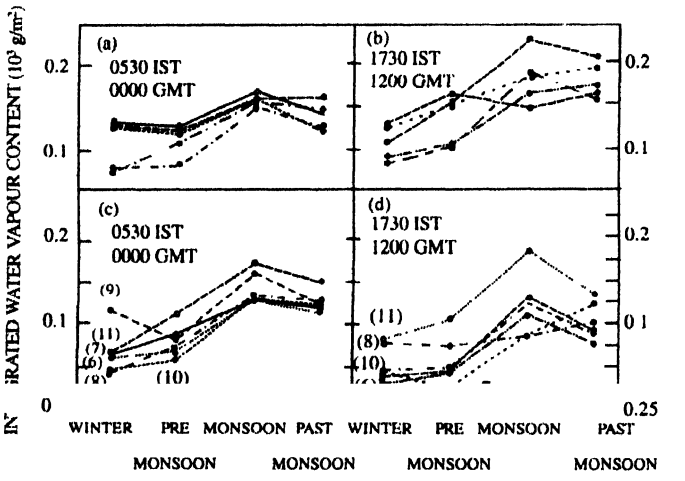

Figure 22. Seasonal variation of attenuation (dB/km) over the Indian subcontinent.

9. Discussion and conclusions

It is understood that the effect of dry air in microwave propagation is quite a stable phenomenon and can be well calibrated for specific purposes. On the other hand, the effect due to water vapour is highly varying and no surface modelling has been found to be satisfactory.

The investigation with a single frequency at 22.235 GHz for remote sensing of water vapour suffer from being corrupted by tropospheric liquid water droplets in the form of clouds.

This problem may be alleviated by using an additional frequency based on the fact that water vapour and liquid water droplets possess completely dissimilar thermal radiation spectra. However, with the use of dual frequency radiometers for remote sensing of water vapour produces still an error of 1–2 cm at zenith and 4–6 cm at lower elevation angles. This problem is alliviated by Menius *et al* [44], Westwater [45] and Gaut [46] by adopting a linear combination of three frequency radiometric studies on water vapour. But still this suffers from error. This, again, however be alleviated by 'linearising' the brightness temperature [47].

References

[1] J V Evans and T Hagfors *Radio Astronomy* (New Delhi : McGraw Hill) (1998)

[2] J H Van Vleck and V F Weisskopf *Rev. Mod. Phys.* **17** 227 (1954)

[3] E P Gross *Phys. Rev.* **97** 395 (1955)

[4] S A Zhevakin and A P Nanmov *Izv. Vuz. Radiofizika* **6** 674 (1963)

[5] P W Rosenkranz *IEEE Trans.* **AP-23** 498 (1975)

[6] H J Liebe *Radio Sci.* **20** 1069 (1985)

[7] K J Llewellyn-Jones, R J Knight and H A Gebbie *Nature* **274** 876 (1978)

[8] R A Bohlander, R J Emegy, D J Llewellyn-Jones, G G Gimmestad, H A Gebbie, O A Sinpson, J J Gallagher and S Perkowitz in *Atmospheric Water Vapour* (eds) A Deepak *et al* (New York : Academic) p241 (1980)

[9] H R Caslon and C S Harden *Appl. Opt.* **19** 1776 (1980)

[10] S A Clough, F X Kneizys, R Davies, R Gamach and R Tipping *in Atmospheric Water Vapour* (eds) A Deepak *et al* (New York : Academic) p25 (1980)

[11] M E Thomas and R J Nordstrom *J. Quant. Spectrosc. Radiat. Transfer* **28** 103 (1982)

[12] C J Gibbins *Electron. Lett.* **22** 577 (1986)

[13] B R Bean and E J Dutton *Radio Meteorology* (New York : Dover) (1968)

[14] C K Bhattacharya *PhD Thesis* (Benaras Hindu University, Varansi, India) (1985)

[15] P K Karmakar, S Chattopadhyay and A K Sen *Int. J. Remote Sensing* (UK) **20** 2637 (1999)

[16] J E Allnult *Proc. IEEE* **123** 1197 (1976)

[17] A Mitra, P K Karmakar and A K Sen *Indian J Phys.* **74B** 379 (2000)

[18] M K Raina *Indian J. Radio Space Phys.* **17** 129 (1988)

[19] J M Moran and B R Rosen *Radio Sci.* **16** 235 (1981)

[20] S Chattopadhyay *PhD Thesis* (Calcutta University, India) (1996)

[21] H J Liebe *Int. J. Infrared and Millimeterwaves* **10** 631 (1989)

[22] J W Waters *Methods of Experimental Phyics* (ed) M L Meeks (New York : Academic) **Vol. 12** part-B (1976)

[23] A K Sen, P K Karmakar, A Mitra, A K Davgupta, P K Chakraborty, S Devbarman and T K Das *Int. J Remote Sensing* **10** 1119 (1989)

[24] E R Westwater and M T Dechen *Inversion Methods in Atmospheric Remote Sounding* (New York : Academic) p395 (1977)

[25] D C Hogg, F O Guiraud, J B Snider, M T Decker and F R Westwater *J. Climate Appl. Meteorol.* **22** 789 (1983)

[26] E R Westwater *ESSA Tech. Report* IER-30-ITSA 30 (National Technical Information Service, Spring Field, Virginia) (1967)

[27] M L Meeks and A E Lilley *J. Geophys. Res.* **68** 1683 (1963)

[28] G M Resch *TDA Progress Report* (October-December) (1983)

[29] S K Dutta and A K Sen *Int. J. Remote Sensing* **15** 2176 (1994)

[30] M T Decker, E R Westwater and F O Guiraud *J. Appl. Meteorol.* **17** 1788 (1978)

[31] P K Karmakar, A Mitra, M K Sengupta, Ajoy K Dutta and A K Sen *J. Sci. Indus. Res.* (India) **53** 267 (1994)

[32] S N Ghosh and H D Edward *Air Froce Surveys in Geophysics* No. 82 (AF Cambridge Research Center, Tech. Report : AFCRC TN-56-202, AD 98763, USA) (1956)

[33] N C Grody *IEEE Trans. Antennas and Propagation* **AP-24** 155 (1976)

[34] C J Gibbins *J. Inst. Electronic and Radio Engg.* **58** (supplement) 229 (1988)

[35] A Mitra *PhD Thesis* (Calcutta University) (2000)

[36] T F Ulaby, R K Moore and A K Fung *Microwave Remote Sensing, Fundamentals and Radiometry* (Lonodn : Addison-Wisley) **Vol. 1** (1981)

[37] E R Westwater and M T Decker *Atmospheric Water Vapour* (eds) A Deepak *et al* (New York : Academic) p395 (1977)

[38] A K Sen, P K Karmakar, A K Devgupta, A Mitra, J S Sehra and S N Ghosh *Int. J. Remote Sensing* (U.K.) **vol. 9** p1259 (1988)

[39] D M Dension *Rev. Mod. Phys.* **12** 175 (1940)

[40] W S Benedict and L D Kaplan *J. Chem. Phys.* **30** 385 (1959)

[41] D L Croom *J. Atmos. Terres. Phys.* **27** 235 (1965)

[42] J W Waters *Absorption and Emission by Atmospheric Gases in Methods of Experimental Physics* **Vol. 2** Astrophysics-Part B : Radio Telescopes (ed) M L Meeks (New York : Academic) p142 (1976)

[43] A K Sen and P K Karmakar *Indian J. Radio Space Phys.* **17** (1988)

[44] A C Menius, C F Martin, W M Layson and R S Flagg *Tech. Staff. Tech. Memo.* **19** (ETV-TM-64-12, Pan American Airways, Nov. 16) (1994)

[45] E R Westwater *Tech. Report.* (IER30-ITSA30 Environmental Science Service Administration, U S Dept. of Commerce) (1967)

[46] N E Gaut *Tech. Report 467* (MIT Res. Lab. of Elctronics, Dec. 20) (1968)

[47] S C Wu *IEEE Trans. Antenna and Propagation* **AP-27** No. 2 (1979)

About the Authors

P K Kumakar obtained his M. Sc. degree from Calcutta University, India, in 1979 and Ph. D. degree from Calcutta University in 1990. He is working in the department of Radiophysics and Electronics, Calcutta University since 1988. He has more than 35 number of publications in National and International Journal of repute. He has more than 30 number of conference articles. He has been awarded the Young Scientist Award of URSI in the year 1990. He had been to Remote Sensing Lab, University of Kansas, USA as a visiting scientist. He has also been awarded the South-South Fellowship of TWAS to act as visitng scientist at Centre for Space Sciences, China in the year 1997. His current areas of interest include Microwave/millimeterwave propagation, Microwave remote sensing, Modelling of the atmosphere *etc.*

S Chattopadhyay obtained his B. Tech degree from Calcutta University in 1986 and Ph. D. degree from Calcutta University in 1996. From 1988, he is engaged in the department of Radiophysics & Electronics. Calcutta Unversity. He has 12 number of publications in international and National Journals as well as 10 number of conference publications. His current research includes Microwave/millimeterwave propagation, Microwave remote sensing *etc.*